Supplemental Material to:

Jun Hoe Kim, Seung Beom Hong, Jae Keun Lee, Sisu Han, Kyung-Hye Roh, Kyung-Eun Lee, Yoon Ki Kim, Eui-Ju Choi and Hyun Kyu Song

Insights into autophagosome maturation revealed by the structures of ATG5 with its interacting partners

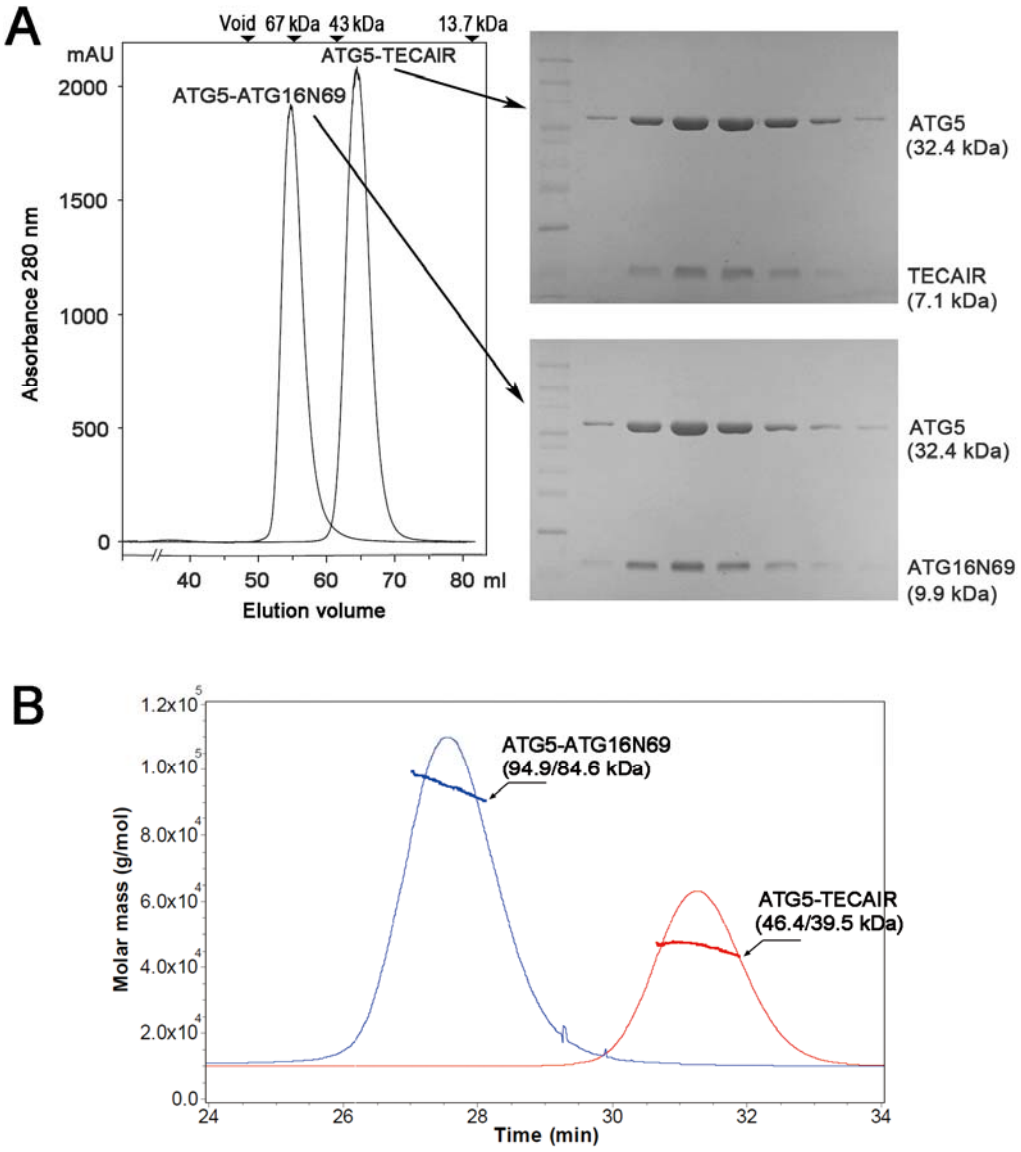

Figure S1. Oligomeric states of ATG5-ATG16N16 and ATG5-TECAIR complexes. (**A**) Gel filtration results for the ATG5-ATG16N69 and ATG5-TECAIR complexes. The elution profile (left) shows that ATG5-ATG16N69 exists as a dimer and ATG5-TECAIR exists as a monomer. SDS-PAGE results (right) confirmed that ATG5-ATG16N69 and ATG5-TECAIR behave as complexes in solution. The calculated molecular masses are shown in parentheses. (**B**) SEC-MALS data of the ATG5-ATG16N69 and ATG5-TECAIR complexes. The average molar masses were determined using the ASTRA V program from UV data obtained with a UPC-9 UV detector and QELS data obtained with a Wyatt MiniDAWN TREOS instrument (dotted lines). Each species is indicated by an arrow with experimental (MALS) and theoretically calculated (calc.) molar-mass values shown in parentheses (MALS/calc.).

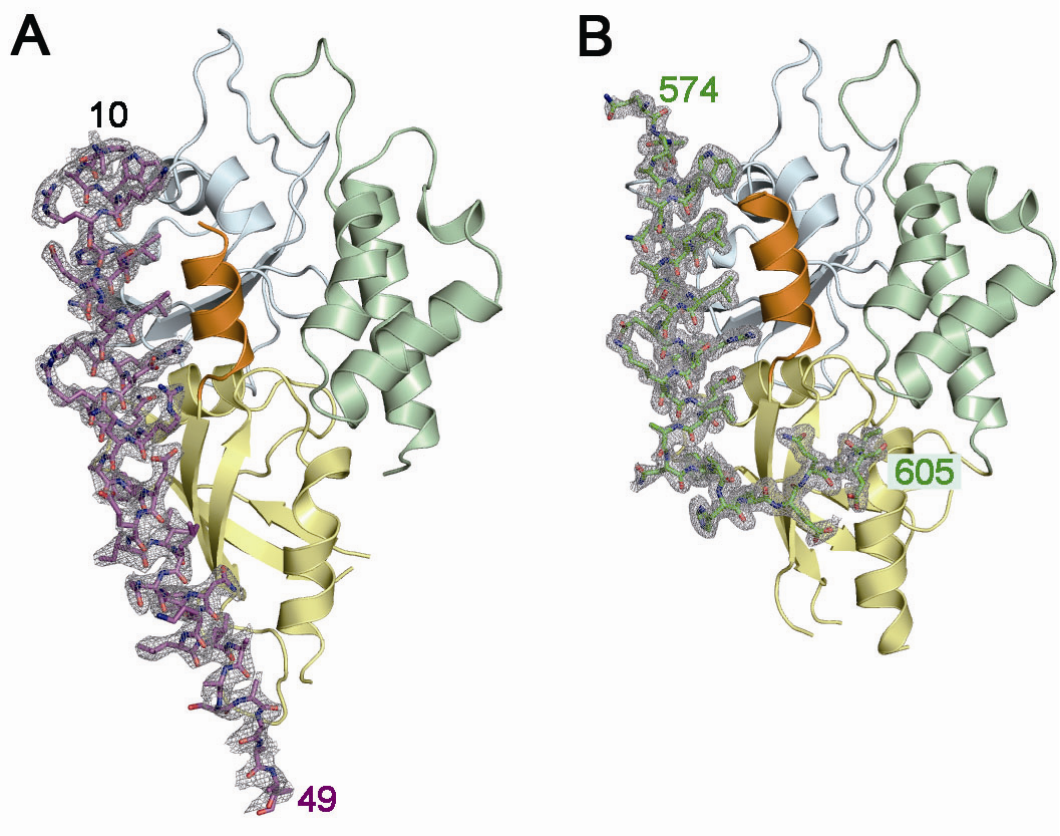

Figure S2. Electron density map of ATG5-binding partners. (**A**) The $2|F_o|-|F_c|$ electron density map of bound ATG16N69 is shown using a mesh surface at the 1.5σ contour level. (**B**) The $2|F_o|-|F_c|$ electron density map of bound TECAIR is shown by a mesh surface at the 1.5σ contour level. The color scheme for ATG5 is as described in **Figure 2**.

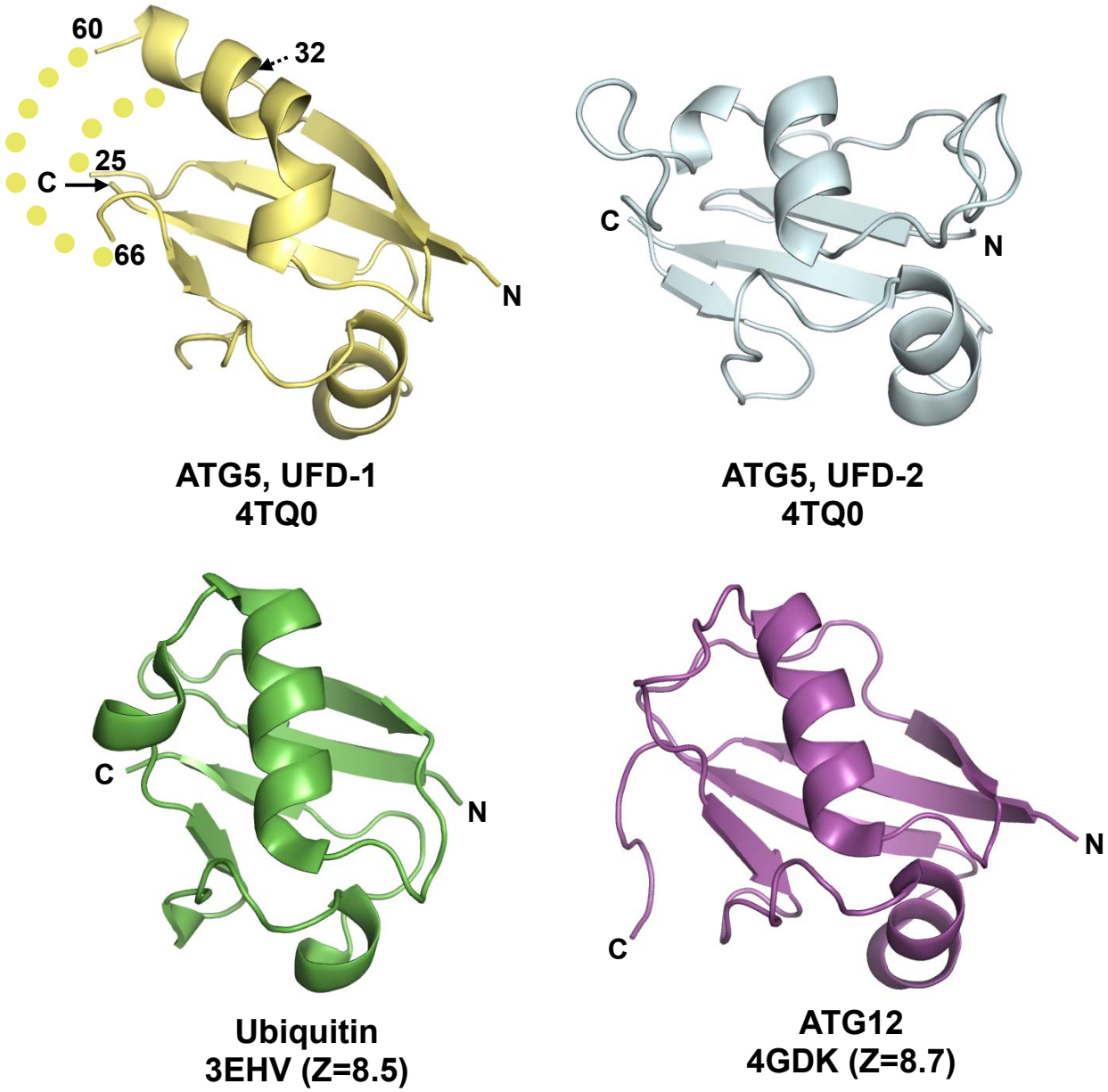

Figure S3. Ribbon diagrams comparing the UFDs of ATG5 with ubiquitin and ATG12. PDB codes and Z-scores from the DALI server are shown below each structure.[1,2] N- and C-termini of each structure are labeled and invisible regions in UFD-1 of ATG5 are drawn as dots. The color scheme for ATG5 is as described in **Figure 2**.

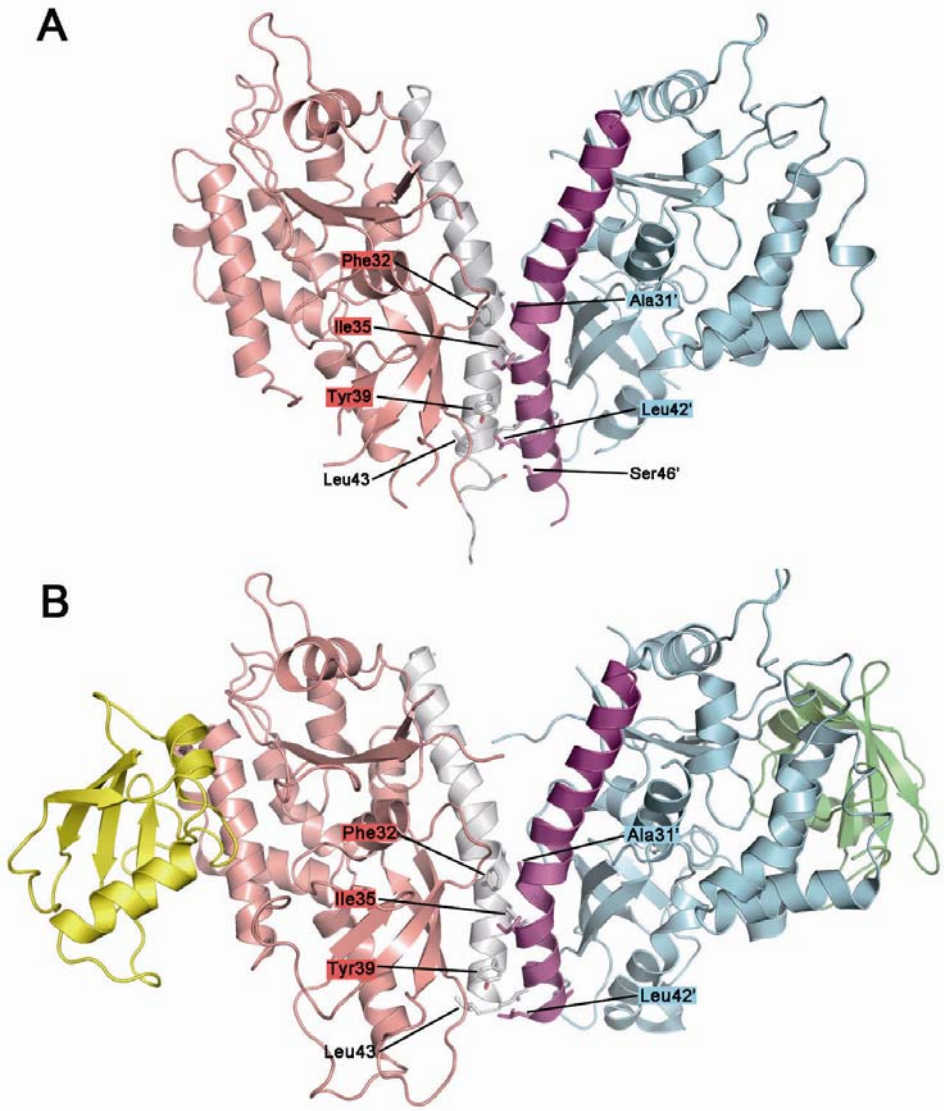

Figure S4. Dimeric structure of ATG16N69. (**A**) Crystallographic dimer structure of the ATG5-ATG16N69 complex. Each ATG5 is colored in salmon and sky blue, respectively, and ATG16N69 is colored gray and purple, respectively. (**B**) Crystallographic dimer structure of the ATG12–ATG5-ATG16N complex which involves a different crystalline packing environment.[2] Colors used for ATG5 and ATG16N69 are the same as panel (**A**) and each ATG12 is colored yellow and green, respectively. The residues involved in the dimeric interface are labeled.

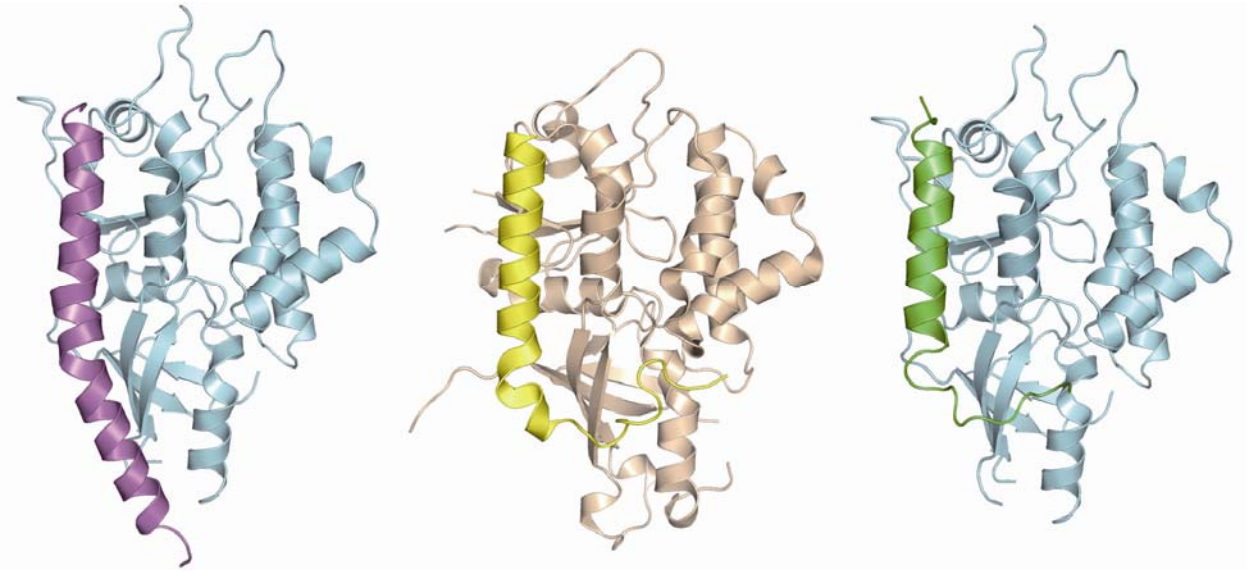

Figure S5. Structural comparisons among human ATG5-ATG16N69 (left), yeast Atg5-Atg16 (middle), and human ATG5-TECAIR complexes (right). The color schemes are the same as in **Figure 3**. The overall structures of ATG5 from human and yeast are quite similar, but the binding mode for the ATG16s from human and yeast is different. Note that the helix/loop ratio in the modeled ATG16 equivalents is 0.9/0.1, 0.69/0.31, and 0.56/0.44 for ATG5-ATG16N69 (left), yeast Atg5-Atg16 (middle), and ATG5-TECAIR complexes (right), respectively.

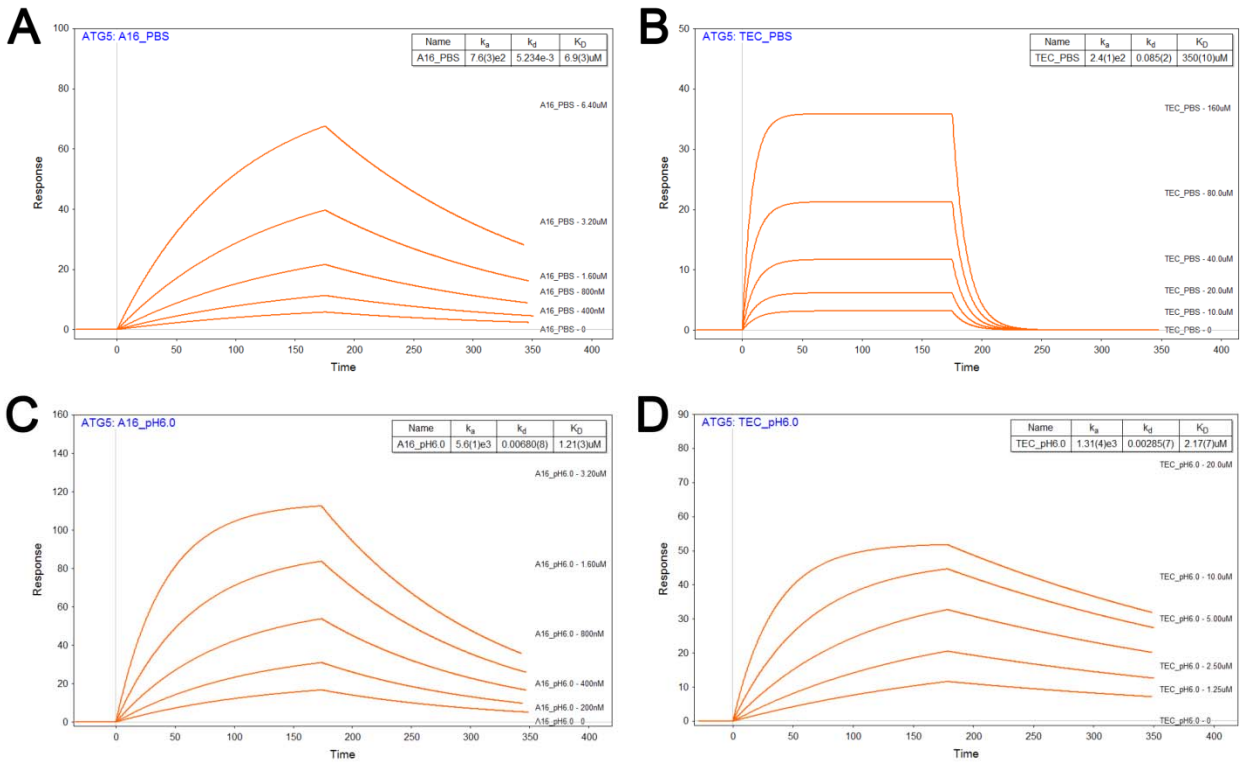

E

Analyte	Buffer pH	Concentration	k_a ($M^{-1}s^{-1}$)	k_d (s^{-1})	K_D (μM)
A16	PBS pH 7.4	200 nM ~ 3.2 μM	$7.6(3)e^2$	$5.234e^{-3}$	6.9(3)
TEC		10 ~ 160 μM	$2.4(1)e^2$	$8.5(2)e^{-2}$	350(10)
A16	Phosphate pH 6.0	100 nM ~ 1.6 μM	$5.6(1)e^3$	$6.80(8)e^{-3}$	1.21(3)
TEC		1.25 ~ 20 μM	$1.31(4)e^3$	$2.85(7)e^{-3}$	2.17(7)

Figure S6. Binding constant measurements by surface plasmon resonance (SPR). The binding of A16 (36 residues from Phe10 to Lys45 of ATG16L1) and TEC (36 residue from Thr575 to Val610 of TECPR1) peptides to immobilized ATG5 were measured under different pH conditions. SPR sensorgrams were recorded using several different concentrations of A16 peptide at pH 7.4 (**A**), TEC peptide at pH 7.4 (**B**), A16 peptide at pH 6.0 (**C**) and TEC peptide at pH 6.0 (**D**). (**E**) Summary of SPR data. The equilibrium dissociation constant (K_D) is obtained by dividing the dissociation rate constant (k_d) by the association rate constant (k_a).

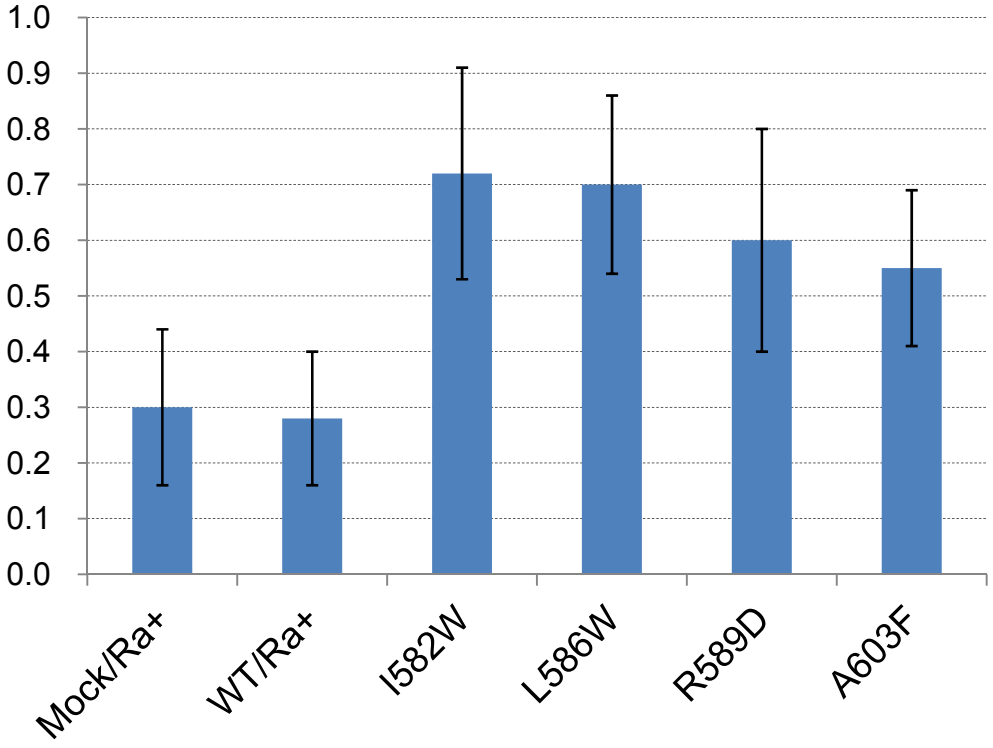

Figure S7. Quantification of TEM images. Ratio of autophagosomes to the total number of autophagosomes plus autolysosomes per cell for the indicated mutants. Approximately 40 cells (from 26 to 48 depending on the particular mutant) were counted per micrograph. The transfected cell populations analyzed by EM in this experiment would contain some cells that expressed exogeneous wild-type or TECPR1 mutants. Hence, it is reasonable to calculate the number of autophagosomes divided by the number of autophagosomes plus autolysosomes with a higher ratio reflecting more defective autophagosome maturation.

Supplementary References

1. Falini G, Fermani S, Tosi G, Arnesano F, Natile G. Structural probing of Zn(II), Cd(II) and Hg(II) binding to human ubiquitin. Chem Comm 2008; 7:5960-52.
2. Otomo C, Metlagel Z, Takaesu G, Otomo T. Structure of the human ATG12~ATG5 conjugate required for LC3 lipidation in autophagy. Nat Struct Mol Biol 2013; 20:59-66.